TRIBUTE TO FOUNDERS: ROY JACKSON. BIOMOLECULAR ENGINEERING, BIOENGINEERING, BIOCHEMICALS, BIOFUELS, AND FOOD

On Facilitated Computation of Mesoscopic Behavior of Reaction-Diffusion Systems

Vu Tran and Doraiswami Ramkrishna
School of Chemical Engineering, Purdue University, West Lafayette, IN 47907

DOI 10.1002/aic.15940
Published online September 28, 2017 in Wiley Online Library (wileyonlinelibrary.com)

Various cellular and subcellular biological systems occur in the conditions where both reactions and diffusion take place. Since the concentration of species varies spatially, application of reaction-diffusion master equation has served as an effective method to handle these complicated systems; yet solving these equation incurs a large CPU time penalty. Counter to the traditional technique of generating many sample paths, this article introduces a method which combines Grima's effective rate equation approach (Grima, J Chem Phys. *2010;133:3) with a linear operator formalism for diffusion to capture averaged species behaviors. The formulation also shows correct results at various choices of compartment sizes, which have been found to be an important factor that can affect accuracy of the final predictions (Erban, Chapman,* Phys Biol. *2009;6:4). It is shown that the method presented allows the computation of the mesoscopic average of reaction-diffusion systems at considerably accelerated rates (exceeding a thousand fold) over those based on sample path averages.* © 2017 American Institute of Chemical Engineers *AIChE J*, 63: 5258–5266, 2017
Keywords: diffusion, computational chemistry, computer simulations (MC and MD), reaction kinetics

Introduction

It is a pleasure to participate in a special journal issue honoring Roy Jackson, an eminent scholar of the chemical engineering profession whose contributions most significantly focused on elegant mathematical treatment of particulate systems noted as much for their complexity of behavior as for their engineering importance. The source of complexity is the interplay of particulate motion in a fluid environment together with physicochemical processes featuring reaction and diffusion. Jackson's research laid the foundation for the mathematical treatment of such systems by contributions to formulation, analysis and computation of system behavior.

While Jackson's concern was with traditional settings, it is our objective to address somewhat similar systems that are more of contemporary interest as well as in need of fresh approaches toward their study. Abstractly, they pertain to particulate entities that are distributed in a multidimensional space comprising both spatial coordinates as well as thermodynamic state variables such as temperature, concentrations and so on. The particulate entities may be either material particles (e.g., catalyst pellets) or living cells in which chemical reaction and physical transport occur together. The system evolves not only through the dynamic behavior of the individual entities but also through change in the number of such entities. The framework required to extract system dynamics is that of general population balances as expounded in Ramkrishna's book.[1] We seek the statistically averaged behavior of the system, a frequent objective of Jackson's endeavors connected with his study of gas–solid dispersions.

We will first inquire into the importance of the problems of interest to this article, and follow up by an explanation of what is distinctive about the methodology essential to solve them. In regard to the first, while a recently published review[2] deliberates a diverse variety of potential applications, we will point here to problems connected with biological signaling processes in which cells exposed to specific signaling molecules initiate a set of intracellular gene-regulatory reactions resulting in the formation of specific proteins. The reader will note that this process represents the very basis of cellular differentiation which transforms stem cells into numerous cell types with characteristic functions. The importance of this application should therefore be evident.

The second issue relates to difficulties associated with the solution of the problems just outlined and how they may be overcome. Signaling in cells often involves a small number of molecules so that the reactions among them occur at a random rate.[3–5] In addition, they follow nonlinear kinetics so that the average behavior does not obey macroscopic kinetics. Thus intracellular balances are (continuous) nonlinear stochastic differential equations whose average behavior must be found by detailed evaluation of sample paths using Monte Carlo simulative algorithms.[6,7] This process becomes forbiddingly tedious for a sizable population of cells with further exacerbation arising from often encountered stiffness of the differential equations. The chemical master equation (CME),[8] affords a natural avenue for formulation of stochastic reaction systems preserving the discrete nature of the numbers of reacting entities. Together with system size expansion techniques,[8,9] CME provides in fact the route to arriving at the continuous

Correspondence concerning this article should be addressed to D. Ramkrishna at ramkrish@purdue.edu.

stochastic differential equations referred to above. However, CME does not inspire computational methodology toward extracting system behavior. Consequently, researchers have been led to use simulation methods such as stochastic simulation algorithm (SSA)[10] (or equivalently the interval of quiescence used by Shah et al.[11]) suitably embellished by "tau-leap" strategies designed to skip events that do not make notable changes to system dynamics.[12–18] In spite of the foregoing armory of techniques, the computation of average behavior of systems of interest to this article has been thwarted by overwhelming demands on computational costs primarily due to the large number of stochastic dynamical equations.

A refreshing approach toward resolving the above dilemma appears in a paper by Grima,[19] which raises the possibility of directly obtaining average (mesoscopic) behavior by entirely circumventing the computation of sample paths. The underlying methodology is grounded in quasi-linearization leading to a derivation of dynamical equations which represent the potential source of average behavior. A demonstration of this approach appears in the recent publication of Smith et al.[20] from Grima's group through a biological example which shows that the average mesoscopic behavior was dependent on the diffusion coefficients connected with random motion. Such behavior is characteristic of growth in biofilms, a research area which motivates our current effort.

The objective of this article is to investigate a stochastic reaction system, comprising n species, in a discrete number of well-stirred cells which are connected by diffusive transport thus coupling the behavior of all reaction cells. The reactions are represented as

$$s_{1,j}X_1+s_{2,j}X_2+\cdots+s_{n,j}X_N \xrightarrow{k_j} r_{1,j}X_1+r_{2,j}X_2+\cdots+r_{n,j}X_n, \quad j=1,2,\ldots,R \tag{1}$$

This scenario is a simplified version of growth in a biofilm in which cells are embedded without accounting for growth or distinction between extra- and intracellular variables. The mass balance equations for each cell account for diffusive mixing from all other cells and a stochastic reaction term in the given cell. Taking expectation of the above equations produces the expectation of the nonlinear reaction terms to which Grima's[19] approximation is made.

While stochastic simulation has been largely restricted to well-mixed stochastic systems, its extension to a system where diffusional effects compete with reaction has been somewhat sporadic. Experiments show that diffusion can also occur at rates comparable with those of reactions[17] thus invalidating the well-mixed assumption. In contrast to a well-mixed stochastic system, studies on spatial stochastic systems have only begun recently and a clear understanding of how to accurately tract them is yet to emerge. Moreover, generation of sample paths by SSA can be utilized to obtain the average number density of species, the true solution. This true solution is assumed to be almost the same or only slightly different from the solution of the CME. Recent studies from Grima's group[19] showed at the mesoscopic limit, the deviation between these two can be significant. His approach to reaction kinetics for small volumes presents a way to handle reaction in this system. This article introduces the concept of applying a discrete self-adjoint linear operator whose spectral representation is used to capture the diffusional effect.

In this article, we attempt to handle this problem in two dimensions by applying two different methods to capture both reactions and diffusion without generating sample paths. The domain of interest is divided into a two-dimensional array of small well-mixed compartments. These compartments are assumed for convenience to be squares of equal size although this assumption is not essential. Reactions occur within each compartment. Concentration of species varies spatially which allows diffusion to occur between neighboring compartments. In the following section, we will briefly discuss the application of the effective mesoscopic rate equations (EMREs)[19] in an effort to approximate the solutions from CME for the reaction system. In the next section, we will provide formulation of the linear operator and its definition, as well as how it can be applied in order to account for the diffusion effect in the system. The results from our current method can be then compared with the results generated by solving the reaction-diffusion master equation.[21–24]

Analysis

The two dimensional domain is divided into discrete squares of length l. Along the "horizontal" and "vertical" coordinate, we have

$i=0,\pm1,\pm2,\ldots,\pm M \quad (2M+1)$ discrete elements.

Denote

$$S^I \equiv \{-M,-M+1,\ldots,-2,-1,0,1,2,\ldots,M\}$$

$j=0,\pm1,\pm2,\ldots,\pm N \quad (2N+1)$ discrete elements. Denote

$$S^J \equiv \{-N,-N+1,\ldots,-2,-1,0,1,2,\ldots,N\}$$

There are n variables each representing particle numbers of reaction species in the cell located at (i,j), denoted $Z_{i,j}^{(s)}$, $s=1,2,\ldots,n$. Define $Z_{i,j}^{(s)} \equiv X_{li,lj}^{(s)}/l$ as the ij^{th} component of scaled vector $\mathbf{Z}$ with $\mathbf{X}$ as the vector the actual particle numbers in the physical domain. Collating every cell in the domain, we may define the vector

$$\mathbf{Z}^{(s)}=\left\{Z_{i,j}^{(s)};\quad i\in S^I; j\in S^J\right\}\in \mathrm{H}\equiv \Re^{2N+1}\otimes\Re^{2M+1}$$

Effective mesoscopic rate equation[19]

The CME in general cannot be solved analytically; however, the dynamics of the reaction system (1) can be captured by means of the system-size expansion due to Van Kampen[8] using

$$\frac{n_i}{\Omega}=\phi_i+\Omega^{-1/2}\varepsilon_i \tag{2}$$

where ϕ_i is the macroscopic concentration of species i as determined by the regular rate equation (RE) and ε_i is a continuous random variable which represents the system-scaled fluctuation in concentration. Grima's analysis[19] arrives at the following equation in the average fluctuation:

$$\frac{d\langle\varepsilon\rangle}{dt}=\mathbf{J}\langle\varepsilon\rangle+\Omega^{-1/2}\Delta(\mathbf{C})+O(\Omega^{-1}) \tag{3}$$

$$\frac{d\mathbf{C}}{dt}=\mathbf{J}\mathbf{C}+\mathbf{C}\mathbf{J}^T+\mathbf{D}+O(\Omega^{-1/2}) \tag{4}$$

where $\langle\varepsilon\rangle\equiv[\,\langle\varepsilon_1\rangle\quad\langle\varepsilon_2\rangle\quad\cdots\quad\langle\varepsilon_n\rangle\,]^T$ is the vector of the first moment,

$\mathbf{J}\equiv\mathbf{S}\nabla_\phi\mathbf{f}(\phi)$ $(n\times n)$ matrix, $\mathbf{f}(\phi)\equiv[f_1(\phi)f_2(\phi)\cdots f_n(\phi)]^T$, $\phi\equiv[\,\phi_1\quad\phi_2\quad\cdots\quad\phi_n\,]$,

$\mathbf{S}\equiv\left\{S_{ij}\equiv\left(s_{ij}-r_{ij}\right);i=1,2,\ldots,n;j=1,2,\ldots,R\right\}$ is an $(n\times R)$ matrix.

Δ is a column vector whose s^{th} entry are the coefficients of $\Omega^{-1/2}$, $\mathbf{C}$ is a symmetric matrix with its ij^{th} coefficient given by $C_{ij} \equiv \langle \varepsilon_i \varepsilon_j \rangle$, where the angular bracket denotes the mean.

$$\Delta \equiv \frac{1}{2}\sum_{k=1}^{n}\left(\sum_{i,j=1}^{n}\frac{\partial J_{ki}}{\partial \phi_j}C_{ij} - \sum_{i=1}^{n}\phi_i\frac{\partial J_{ki}}{\partial \phi_i}\right)\mathrm{e}_k \tag{5}$$

In the above equation $\mathbf{e}_k \equiv [0 \quad \cdots \quad 1 \quad \cdots \quad 0]^T$ is the k^{th} unit (column) vector in $\Re^n$. The notation $\Delta(\mathbf{C})$ in Eq. 3 is used to indicate that the vector Δ is evaluated at $\mathbf{C}$, satisfying Eq. 4, using Eq. 5. From these equations, the average value of each species can be calculated directly without usage of the SSA method for sample paths.

Linear operator for the diffusion

Reactions. We assume R reactions involving the n species. The propensity of the r^{th} reaction occurring in the cell at (i,j) is denoted as $a_r(\mathrm{Z}_{i,j})$. Next, we define stoichiometric matrix $\{\beta_{s,r}; s=1,2,\ldots,n; r=1,2,\ldots,R\}$ so that the rate of change of concentration of each species may be related to the reaction rate vector. Thus we may write the rates of change of concentration of the s^{th} extracellular species in rectangular domain at (i,j) as $\sum_{r=1}^{R}\beta_{s,r}a_r(\mathrm{Z}_{i,j})$.

Mass Balances. We have a set of stochastic processes $Z_{i,j}^{(s)}$ that must be simulated so that their average values $\langle Z_{i,j}^{(s)}\rangle$ can be obtained. The average concentrations must satisfy the differential equations

$$\begin{gathered}\frac{d\langle Z_{i,j}^{(s)}\rangle}{dt} = D_l\left(\langle Z_{i-1,j}^{(s)}\rangle + \langle Z_{i+1,j}^{(s)}\rangle + \langle Z_{i,j-1}^{(s)}\rangle + \langle Z_{i,j+1}^{(s)}\rangle - 4\langle Z_{i,j}^{(s)}\rangle\right) \\ + \left\langle \sum_{r=1}^{R}\beta_{s,r}a_r(Z_{i,j})\right\rangle, \\ s=1,2,\ldots,n; \quad i=0,\pm1,\pm2,\ldots,\pm M-1; j=0,\pm1, \\ \pm2,\ldots,\pm N-1\end{gathered} \tag{6}$$

D_l is the diffusion coefficient for the l^{th} species through the biofilm. The last term on the right hand side is the change in concentration resulting from reactions. For the situation where no variable can escape through the boundaries of the biofilm, we may write the equations for the boundaries as shown below.

$$\begin{gathered}\frac{d\left\langle Z_{-M,j}^{(s)}\right\rangle}{dt} = D_l\left(\left\langle Z_{-M+1,j}^{(s)}\right\rangle + \left\langle Z_{-M,j-1}^{(s)}\right\rangle + \left\langle Z_{-M,j+1}^{(s)}\right\rangle \right. \\ \left. -3\left\langle Z_{-M,j}^{(s)}\right\rangle\right) + \left\langle \sum_{r=1}^{R}\beta_{s,r}a_r(Z_{-M,j})\right\rangle, \\ s=1,2,\ldots,n, \quad j \in S^J\end{gathered} \tag{7}$$

$$\begin{gathered}\frac{d\left\langle Z_{M,j}^{(s)}\right\rangle}{dt} = D_l\left(\left\langle Z_{M-1,j}^{(s)}\right\rangle + \left\langle Z_{M,j-1}^{(s)}\right\rangle + \left\langle Z_{M,j+1}^{(s)}\right\rangle - 3\left\langle Z_{M,j}^{(s)}\right\rangle\right) \\ + \left\langle \sum_{r=1}^{R}\beta_{s,r}a_r(Z_{M,j})\right\rangle, \\ s=1,2,\ldots,n, \quad j \in S^J\end{gathered} \tag{8}$$

$$\begin{gathered}\frac{d\langle Z_{i,-N}^{(s)}\rangle}{dt} = D_l\left(\langle Z_{i-1,-N}^{(s)}\rangle + \langle Z_{i+1,-N}^{(s)}\rangle + \langle Z_{i,-N+1}^{(s)}\rangle - 3\langle Z_{i,-N}^{(s)}\rangle\right) \\ + \left\langle \sum_{r=1}^{R}\beta_{s,r}a_r(Z_{i,-N})\right\rangle, \\ s=1,2,\ldots,n, \quad i \in S^I\end{gathered} \tag{9}$$

$$\begin{gathered}\frac{d\langle Z_{i,N}^{(s)}\rangle}{dt} = D_l\left(\langle Z_{i-1,N}^{(s)}\rangle + \langle Z_{i+1,N}^{(s)}\rangle + \langle Z_{i,N-1}^{(s)}\rangle - 3\langle Z_{i,N}^{(s)}\rangle\right) \\ + \left\langle \sum_{r=1}^{R}\beta_{s,r}a_r(Z_{i,N})\right\rangle, \\ s=1,2,\ldots,n, \quad i \in S^I\end{gathered} \tag{10}$$

Operator Formulation. Equations 6–10 for each s may be succinctly written by defining the following operators.

$$\begin{gathered}\mathbf{L}^I : \Re^{2M+1} \to \Re^{2M+1}, \quad \mathbf{L}^J : \Re^{2N+1} \to \Re^{2N+1}, \\ \mathbf{I}^I \equiv \text{ Identity on } \Re^{2M+1}, \mathbf{I}^J : \text{Identity on } \Re^{2N+1} \\ \mathbf{T} \equiv \left(\mathbf{L}^I \otimes \mathbf{I}^J + \mathbf{I}^I \otimes \mathbf{L}^J\right) : \left(\Re^{2M+1} \otimes \Re^{2N+1}\right) \\ \to \left(\Re^{2M+1} \otimes \Re^{2N+1}\right)\end{gathered}$$

where

$$\mathbf{L}^I \equiv \underset{(2M+1)\times(2M+1)}{\begin{bmatrix} -2 & 1 & 0 & \cdots & & & & 0 \\ 1 & -2 & 1 & 0 & \cdots & & & 0 \\ 0 & 1 & -2 & 1 & 0 & \cdots & & 0 \\ \vdots & \vdots & \vdots & & & & & \vdots \\ & & & & & & & \\ & & & & & & & 0 \\ 0 & \cdots & & & & 1 & -2 & 1 \\ 0 & & & & \cdots & 0 & 1 & -2 \end{bmatrix}},$$

$$\mathbf{L}^J \equiv \underset{(2N+1)\times(2N+1)}{\begin{bmatrix} -2 & 1 & 0 & \cdots & & & & 0 \\ 1 & -2 & 1 & 0 & \cdots & & & 0 \\ 0 & 1 & -2 & 1 & 0 & \cdots & & 0 \\ \vdots & \vdots & \vdots & & & & & \vdots \\ & & & & & & & \\ & & & & & & & 0 \\ 0 & \cdots & & & & 1 & -2 & 1 \\ 0 & & & & \cdots & 0 & 1 & -2 \end{bmatrix}}$$

The above are symmetric, tridiagonal (Jacobi) matrices with real eigenvalues and orthogonal eigenvectors. Note further that if we had chosen different sizes for the discrete reaction domains, we would still have a self-adjoint operator.[25] Denoting the eigenvalues and eigenvectors of $\mathbf{L}^I$ and $\mathbf{L}^J$ by

$$\left\{\lambda_i^I,\ \mathbf{z}_i^I;\quad i\in S^I\right\},\ \left\{\lambda_j^J,\ \mathbf{z}_j^J;\quad j\in S^J\right\}$$

they are identified (see Amundson[26]) as

$$\lambda_i^I=-2\left(1+\cos\frac{\pi(i+M)}{2(M+1)}\right),\quad i\in S^I$$

$$\mathbf{z}_i^I=\left[\sum_{k=1}^{2M+1}\left(\frac{\sin\left[\pi(i+M+1)k/(2M+2)\right]}{\sin\left[\pi(i+M+1)/(2M+2)\right]}\right)^2\right]^{1/2}\times\begin{bmatrix}\dfrac{\sin\left[\pi(i+M+1)(2M+1)/(2M+2)\right]}{\sin\left[\pi(i+M+1)(2M+2)\right]}\\ -\dfrac{\sin\left[\pi(i+M+1)(2M)/(2M+2)\right]}{\sin\left[\pi(i+M+1)(2M+2)\right]}\\ \dfrac{\sin\left[\pi(i+M+1)(2M-1)/(2M+2)\right]}{\sin\left[\pi(i+M+1)(2M+2)\right]}\\ \vdots\\ \vdots\\ (-1)^{2M}\end{bmatrix}$$

$$\lambda_j^J=-2\left(1+\cos\frac{\pi(j+N)}{2(N+1)}\right),\quad j\in S^J$$

$$\mathbf{z}_j^J=\left[\sum_{k=1}^{2N+1}\left(\frac{\sin\left[\pi(j+N+1)k/(2N+2)\right]}{\sin\left[\pi(j+N+1)/(2N+2)\right]}\right)^2\right]^{1/2}\times\begin{bmatrix}\dfrac{\sin\left[\pi(j+N+1)(2N+1)/(2N+2)\right]}{\sin\left[\pi(j+N+1)(2N+2)\right]}\\ -\dfrac{\sin\left[\pi(j+N+1)(2N)/(2N+2)\right]}{\sin\left[\pi(j+N+1)(2N+2)\right]}\\ \dfrac{\sin\left[\pi(j+N+1)(2N-1)/(2N+2)\right]}{\sin\left[\pi(j+N+1)(2N+2)\right]}\\ \vdots\\ \vdots\\ (-1)^{2N}\end{bmatrix}$$

The operator $\mathbf{T}$ is readily shown to be self-adjoint relative to the regular inner product in H given by $\langle\mathbf{u}^I\otimes\mathbf{u}^J,\mathbf{v}^I\otimes\mathbf{v}^J\rangle=\langle\mathbf{u}^I,\mathbf{v}^I\rangle_I\langle\mathbf{u}^J,\mathbf{v}\rangle_J$, where subscripts I and J are used to represent the regular inner products in $\Re^{2M+1}$ and $\Re^{2N+1}$, respectively. The self-adjointness of $\mathbf{T}$ follows from that of $\left(\mathbf{L}^I\otimes\mathbf{I}^J\right)$ and $\mathbf{I}^I\otimes\mathbf{L}^J$. We show the self-adjointness of $\left(\mathbf{L}^I\otimes\mathbf{I}^J\right)$ below.

$$\begin{aligned}\langle\left(\mathbf{L}^I\otimes\mathbf{I}^J\right)(\mathbf{u}^I\otimes\mathbf{u}^J),\mathbf{v}^I\otimes\mathbf{v}^J\rangle&=\langle\left(\mathbf{L}^I\mathbf{u}^I\otimes\mathbf{u}^J\right),\\ \mathbf{v}^I\otimes\mathbf{v}^J\rangle&=\langle\mathbf{L}^I\mathbf{u}^I,\mathbf{v}^I\rangle_I\langle\mathbf{u}^J,\mathbf{v}^J\rangle_J\\ =\langle\mathbf{u}^I,\mathbf{L}^I\mathbf{v}^I\rangle_I\langle\mathbf{u}^J,\mathbf{v}^J\rangle_J&=\langle(\mathbf{u}^I\otimes\mathbf{u}^J),\left(\mathbf{L}^I\mathbf{v}^I\otimes\mathbf{v}^J\right)\rangle\\ =\langle\mathbf{u}^I\otimes\mathbf{u}^J,\left(\mathbf{L}^I\otimes\mathbf{I}^J\right)(\mathbf{v}^I\otimes\mathbf{v}^J)\rangle&\end{aligned}$$

The self-adjoint projections of $\mathbf{T}$ are given by

$$\left(\mathbf{P}_i^I\otimes\mathbf{P}_j^J\right)()=\langle\mathbf{z}_i^I,()\rangle_I\langle\mathbf{z}_j^J,()\rangle_J$$

Spectral Representation of T and Its Functions.

$$\mathbf{T}=\sum_{i=-M}^{M}\sum_{j=-N}^{N}\left(\lambda_i^I+\lambda_j^J\right)\left(\mathbf{P}_i^I\otimes\mathbf{P}_j^J\right)$$

Since in the sequel, it would be necessary to obtain $e^{\mathbf{T}}$, we identify it as

$$e^{\mathbf{T}}=\sum_{i=-M}^{M}\sum_{j=-N}^{N}e^{\left(\lambda_i^I+\lambda_j^J\right)}\left(\mathbf{P}_i^I\otimes\mathbf{P}_j^J\right)$$

Toward Stochastic Simulation. The differential Eqs. 6–9 can be concisely written as

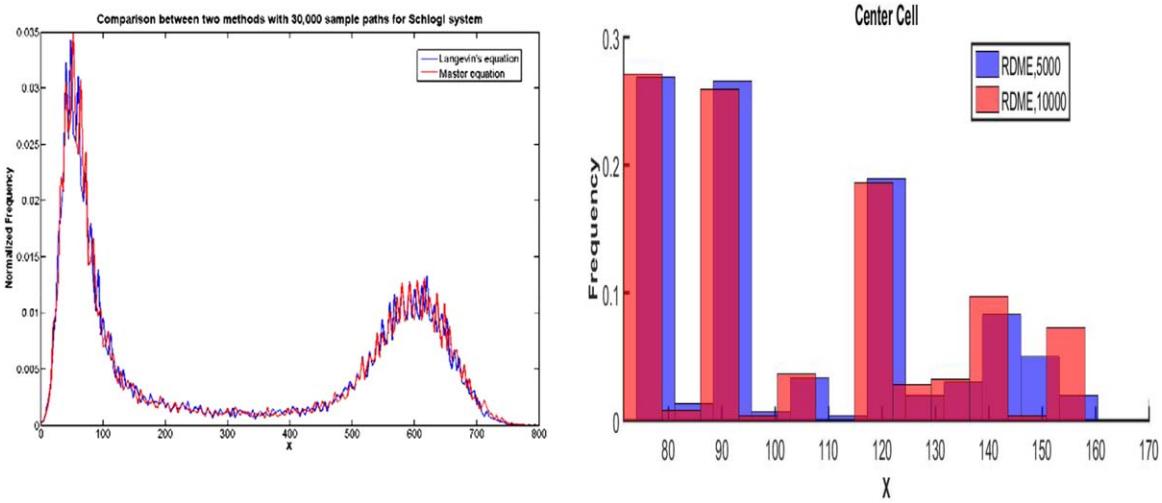

Figure 1. Schlogl's system (a) Distribution of X in the case of single cell simulation and (b) Distribution of X in the center compartment in reactive diffusive system.

[Color figure can be viewed at wileyonlinelibrary.com]

$$\frac{d\langle \mathbf{Z} \rangle}{dt} = \mathbf{DT}\langle \mathbf{Z} \rangle + \langle \mathbf{Ba}(t) \rangle \tag{11}$$

where $\mathbf{B} \equiv \{\beta_{sr};\ s=1,2,\ldots,n;\ r=1,2,\ldots,R\}$; $\mathbf{a} \equiv [a_1\ a_2\ \cdots\ a_R]^T$. It is readily shown that the operator $\mathbf{DT}$ is self-adjoint with respect to the inner product $[\mathbf{u},\mathbf{v}] \equiv \langle \mathbf{D}^{-1}\mathbf{u},\mathbf{v} \rangle$ where $\langle , \rangle$ is the inner product with respect to which $\mathbf{D}$ and $\mathbf{T}$ are both self-adjoint.

The foregoing differential equation is to be integrated from $t=\tau_p$, where τ_p is the p^{th} discrete time. Equation 11 may be integrated subject to the value of $\langle \mathbf{Z}(\tau_p) \rangle$. The solution may be written as

$$\langle \mathbf{Z}(t) \rangle = e^{(t-\tau_p)\mathbf{DT}} \langle \mathbf{Z}(\tau_p) \rangle + \int_{\tau_p}^{t} e^{(t'-\tau_p)\mathbf{DT}} \langle \mathbf{Ba}(t') \rangle dt' \tag{12}$$

The first term on the right side of the above equation captures the change in species due to diffusion occurring between neighboring compartments and the second term describes the change in particle numbers as the result of reactions. The second term on the right hand side of Eq. 12 becomes difficult to solve as the system involves high order reactions. Grima's EMRE method,[19] briefly discussed in the earlier section, provides a tool to compute this average change and hence complete the full calculations for this reactive-diffusive system.

Kullback-Leibler Divergence. Kullback-Leibler divergence is a measure of how one probability distribution diverges from an expected probability distribution.[27–29] In a general case, a calculated divergence of 0 indicates no difference detected between the two distribution, whereas, Kullback-Leibler divergence of 1 indicates that the two distributions behave in totally different manner and can conclude they have no relationship to one another. The measurement can apply to both discrete random variables and continuous random variables. In our case, we will use the discrete version shown in Eq. 13 below:

$$D_{KL}(p(x)||q(x)) = \sum_{x \in X} p(x)\ \ln \frac{p(x)}{q(x)} \tag{13}$$

where $p(x)$ is the expected probability distribution and $q(x)$ is probability distribution which is used to estimate $p(x)$.

Examples

Diffusion augmented Schlogl's system

The well-known system Schlogl has been well studied and used widely to illustrate new simulation algorithms. The system involves two reversible stochastic relations and the environment can be assumed to be well-mixed. Here in this article, we attempted to expand the system and allow diffusion to occur within the domain of interest. We also perturb the conditions slightly so that we can still relate our simulation results for the diffusive reactive system with that of the original single cell case. The Schlogl's chemical reaction model is shown in Ref. 14. This model is noted for its bistability. B_1 and B_2 are constants with their particle numbers as N_1 and N_2, respectively

$$B_1 + 2X \underset{c_2}{\overset{c_1}{\rightleftarrows}} 3X, \quad B_2 \underset{c_4}{\overset{c_3}{\rightleftarrows}} X$$

The values of (dimensionless) parameters, adapted from Cao et al.,[11] are $c_1 = 3\times10^{-7}$, $c_2 = 10^{-4}$, $c_3 = 10^{-3}$, $c_4 = 3.5$, $N_1 = 1\times10^5$, and $N_2 = 2\times10^5$. The initial condition of X is 250 and we simulate the system up to $t=4$.

For this application, we allow the same set of reactions to occur within each squared sub-domain and the diffusion between different neighbor sub-units. Also the particle numbers of B_1 and B_2 in the bulk surrounding the domain is maintained to be the same as those in the single cell case. We set the particle numbers of all species in all compartments to be zero and set diffusivity to be 0.1.

Bimolecular reactions-two model problems

This is a hetero-reaction which involves two species A and B. The example is subjected to two reactions below:

$$A + B \xrightarrow{k_1} B, \qquad \varnothing \xrightarrow{k_2} A$$

In the first reaction, B acts as a catalyst for the decay of A. The second reaction is coupled with the first and represents the generation of A. If we denote a the area of the cell. The values for parameters are $k_1/a = 0.2s^{-1}$, $k_2 a = 1s^{-1}$, $A(0)=5$, and $B(0)=1$.

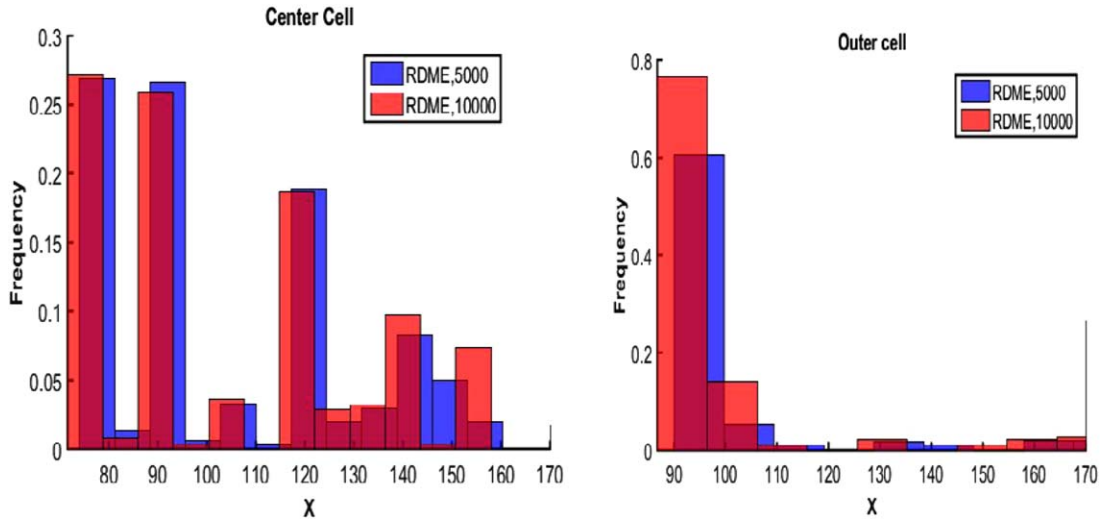

Figure 2. Distribution of X in (a) center compartment and (b) outer compartment.

[Color figure can be viewed at wileyonlinelibrary.com]

Discussion

Two main examples have been utilized to illustrate how effectively the proposed method works. The first example is the diffusion augmented Schlogl's system. Figure 1a shows the distribution of X at $t=4$ by applications of two different approaches: Langevin's equation[30–32] and Master equation with 30,000 sample paths each. The figure shows a well-known feature of this system, the bi-modal distribution. In Figure 1b, we have shown the distribution X in the central compartment of the domain using RDME.

From the figure, there is not much difference between two distributions, coming from 5000 sample-path vs. 10,000 sample-path simulations. The number of sample paths is significantly lower than that in the case of the single cell as the time step is chosen to be the smallest of those generated for all the compartments. This lower time step reduces the error in the propensity function due to its being fixed during the time interval. This comparison suggests that beyond 5000 sample paths, simulation produces no significant difference in X distribution. The first interesting feature from this figure is that the particle number is a lot lower as compared to that in the single cell case. All inner compartments have all species set to be zeros initially. As a result of that, there is only diffusion for some period of time through which the materials are transferred from the bulk to the inner cells. Reactions first take place at the outer regions of the domain and subsequently in the inner regions as diffusion occurs and transfers materials from the periphery to the interior. Specifically, in the center compartment, there is no species initially thus nothing occurs until much later, and this explains why the particle number of X is much lower in this case. Another aspect of this plot is that even though the range of X is reduced, the bimodal nature of the distribution of X (observed in the single cell case) is retained. This is a consequence of our choice of boundary and initial conditions. In other words, fixing the bulk concentrations in the exterior, provides for some uniformity with time because of diffusion thus approaching the single cell circumstance. The center cell is also located at the position that is most symmetric spatially, hence receives the most steady supply of particles from all directions because of diffusion. Consequentially, X distribution in this case retains the bimodality observed in the single cell case. To illustrate further, consider Figure 2b which shows the X distribution in a compartment located in the outer-most layer.

Unlike the previous case shown in Figure 2a, the distribution shows no bimodal distribution for which our hypothesis is as follows. Due to the gradient in concentration between the bulk (source) and inner compartments (sink), there is a continuous flow-in and flow-out which gives rise to a very different set of conditions, as compared to the single cell case. On top of it, concentration of species in neighboring compartments is not uniform, differentiating this case from the previous case of the center compartment where the concentration of species around the compartment is relatively uniform. We have also performed Kullback-Leibler divergence for both cases of the center cells and the outer cell. The calculation of the KL divergence is straightforward when we have the same set of data with different frequencies for the two distributions. In our case, since stochastic simulations can provide different values from each sample path, two obtained data are composed of values that are similar but not exact. As a result, the

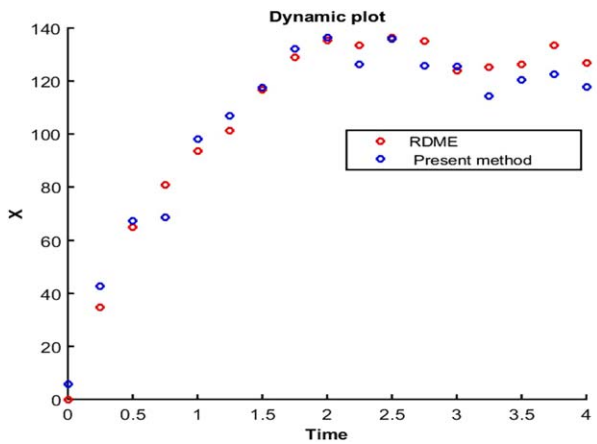

Figure 3. Dynamic plot of averaged X in the center compartment.

[Color figure can be viewed at wileyonlinelibrary.com]

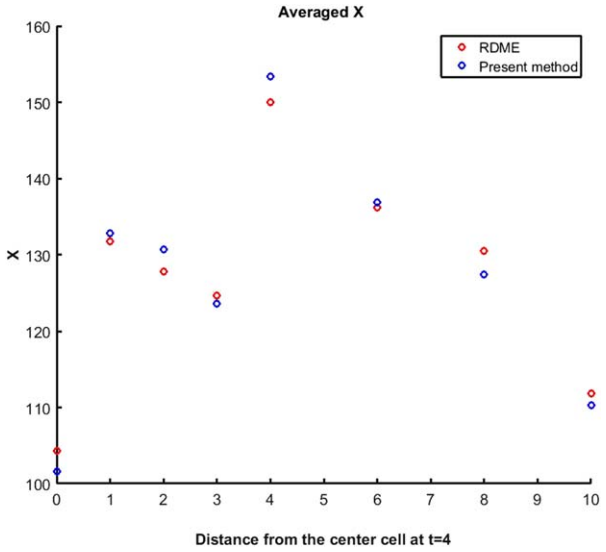

Figure 4. Averaged value of X at different locations.

[Color figure can be viewed at wileyonlinelibrary.com]

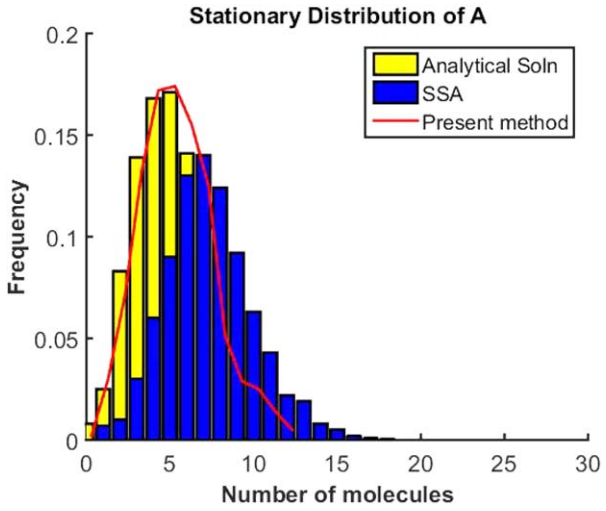

Figure 6. Stationary distribution of *A* in the reactive diffusive system.

[Color figure can be viewed at wileyonlinelibrary.com]

calculations are modified as follows. Instead of looking at each specific value and its corresponding frequency, we chose to compare the total frequency of a small range of values. Specifically for this example, we selected the range to be 2. Also, $\varepsilon = 0.0001$ is chosen to assign to the range of values which is available for one data set and not the other. The KL divergence for the center compartment and the outer compartment shown in Figure 2 are 0.0646 and 0.0869, respectively. Both values indicate even with only 5000 samples paths, the obtained distributions can capture around 92% or better of that from 10,000 sample paths. In Figure 3, we compare the averaged value of X in the compartment located at the center of the domain at different time points generated from two different method: RDME method (10,000 sample paths) and our method.

The average value of X can be calculated as the sum of all products between X value collected from all realization and its corresponding frequency. The data points generated from our methods show close prediction to those simulated by RDME. The averaged relative error from all these points is only 0.12. To further investigate the validity of our approach, we now fix the final time point $t=4$ and vary the positions. Figure 4 shows

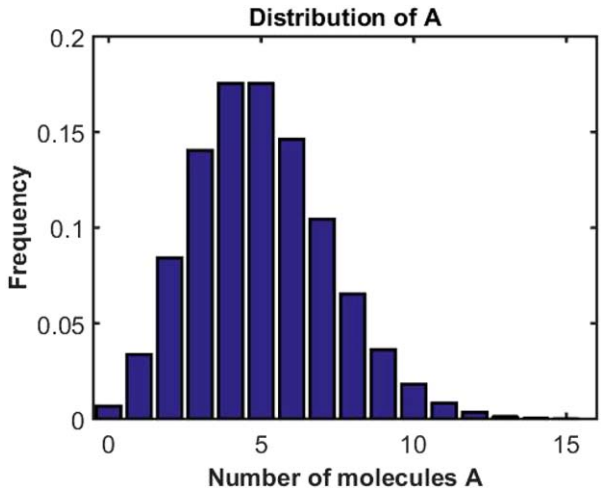

Figure 5. Stationary distribution of A.

[Color figure can be viewed at wileyonlinelibrary.com]

the average value of X at different compartments within the whole domain.

Horizontal axis indicates how many cell units that are between the compartment of interest and the center compartment. The two methods produce close predictions for the averaged value of X at various compartments within the domain. An interesting phenomenon, shown in Figure 4, has been observed in this reaction diffusion system. There is a jump in X between the cells located at the positions that are three units and four units away from the center cell. Figure 4 shows the average value of X at $t = 4$ of different cells located at different positions with respects to the center compartment. The value of X at each specific location on the plot is calculated as the average value from all the compartments that have the same distance to the center compartment. Due to the nature of how the initial conditions and boundary conditions were chosen as well as the diffusion effect, value of X is not necessarily diminishing monotonically with respect to the distance. We fixed the concentration of B1 and B2 in the bulk surrounding the domain to be the same as in the single cell case and zeros everywhere in the inside of the domain initially. We then allowed the diffusion to transfer the materials throughout the domain. Because of that, reactions first take place at the outer regions of the domain and subsequently in the region as diffusion occurs and transfers materials from the periphery to the interior. There are two main effects we have observed here. Reactions occur to generate more X and diffusion transfer the materials between compartments. Initially reactions only occur close to the exteriors but diffusion carries both reactants and products to the interior. At each time point, there are some compartments located inside that gain X both from reactions and the diffusion from the exterior side and so can break the general trend that we would expect. For the specific time point $t = 4$ those specific cells that gain the double effect mentioned above are located around four "compartments" away from the center cell.

The averaged relative error is calculated to be 0.09. The current algorithm outperforms the RDME in term of CPU time. The simulation time for the present method is equivalent with the amount of time it would take the RDME to simulate three trajectories.

The second example is adopted from Ref. 33 except that we modify the rate constant unit and diffusivity unit for reactions and diffusion since our results are simulated for the domain in two dimensions. Similar to the derivation in Ref. 33 the solution for the master equation in the well-mixed case can be solved analytically in the similar manner and arrives as:

$$\phi(n)=\frac{1}{n!}\left(\frac{k_2a^2}{k_1B_0}\right)^n\exp\left[-\frac{k_2a^2}{k_1B_0}\right],$$

where the term on the left indicates the probability that there are n molecules of A in the system. Figure 5 shows the distribution of A from generating 10,000 sample paths in SSA method and it is confirmed to have the same results as from Eq. 13.[33]

For example 2, the whole domain is composed of 21x21 compartments. $D_A=D_B=1(\mu m)^2s^{-1}$, L=1 μm, $k_1=0.2(\mu m)^{-2}s^{-1}$, $k_2=1(\mu m)^{-2}s^{-1}$. Within any compartment (i,j), the propensity function for the reactions can be computed according to:

$$\alpha_{ij,1}(t)=k_1A_{ij}(t)B_{ij}(t)/l^2,\quad \alpha_{ij,2}(t)=k_1l^2.$$

where l^2 is the area of each compartment. In a similar manner, we can write the propensity function for the diffusion of A and B as $A_{ij}D_A/l$ and $B_{ij}D_B/l$. Also, we find the ratio between the propensity function of diffusion to that of reaction to be about 100, indicating that diffusion is a lot quicker than reactions in this case. In Figure 6, we present the three main distributions: the stationary distribution generated from Eq. 13, the distribution generated from the usage of SSA when the domain is divided into 21 $\times$ 21 compartments, and the distribution generated by our present method. We denote them as distribution (I), distribution (II), and distribution (III), respectively. In Erban et al.,[33] he discussed scenarios where the SSA might not be able to capture accurate behaviors of the system. The article further discussed criteria for choosing the appropriate size of each compartment. This development incorporated the effect of diffusivity to the selection of compartment size. He called the new algorithm as an improved SSA and successfully shown that this new algorithm predicts very closely the analytical solution. In our comparison, we compared results generated from the analytical solution, the regular SSA and our present method.

Distribution (II) shifts to the right as compared to the first distribution. This movement has been discussed in the work of Isaacson[24]: in the theoretical limit $l\rightarrow 0$, the bimolecular reaction $A+B\rightarrow\phi$ is lost and the compartment model can only recover the diffusion part. In the example, the second reaction is a zero-th order reaction and so can be computed in term of a total production of A in the whole domain, which is independent of choice l. The bimolecular reaction, conversely, is a second order reaction and hence its rate of consumption of A decreases as l is reduced. These two effects result in a larger amount of A at the end of the process in the domain. Generally, there is an agreement in the literature that there is a bound on l so that $l\gg k_1/(D_A+D_B)$.[24,34] That also explains why when l becomes small, the regular SSA might not necessarily predict accurately the behavior of this system. However, distribution III generated by our method produces similar prediction to the stationary distribution I. KL divergence measurement is used to compare among distribution shown in Figure 6. Similar to the previous example, we selected the range of each period to be 2 and epsilon to be 0.001. The measurement of the KL divergence for the distribution generated by our present method and that by the regular SSA with respect to the distribution generated by the analytical solution are 0.0358 and 0.623. Both Figure 6 and KL measurement indicate that our method can overcome the problem associated with the selection of compartment size. In this example, the simulation time for the present algorithm is as small as it would take for the SSA to complete on two independent trajectories.

Conclusion

This article introduces an algorithm which is capable of capturing the average behaviors of chemical/biological species in a reactive-diffusive system without generating multitudes of sample paths. The method combines EMRE[19] and Linear Operator techniques to describe reaction and diffusion effects simultaneously. Two examples have been used to illustrate the validity of the method. Predictions generated by this algorithm show good agreement with the SSA and require a much lower CPU time for simulations. Extension of this method to larger systems involving many species appears to be feasible. As mentioned in Grima et al.,[19] the algorithm was developed and tested only on simple systems which are composed of a small number of low order reactions. Complex systems with nonlinear reactions can also affect the accuracy of the approximations performed by present method. Also, since the original method of Grima is assumed to work only for well-mixed systems, the value of time step needs to be chosen so that it is not too large to violate that condition yet not too small so that it may take too long to simulate the algorithm. Additional effort on finding criteria for optimal time steps by and capturing accurate behaviors of complex non-linear systems are all considered as future work for this present algorithm. To find the optimal time step, the trial and error method can be used as the initial step but full investigations on how the relative rate between diffusion and reactions in each system might provide the right choice of picking an optimal time step.

Acknowledgment

This work was supported by National Institutes of Health Grant GM081888 (to Wei-Shou Hu).

Literature Cited

1. Ramkrishna D. *Population Balances*. Elsevier, 2000.
2. Ramkrishna D, Singh MR. Population balance modeling: current status and future prospects. *Annual Rev Chem Bimol Eng*. 2014;5:123–146.
3. McAdams HH, Arkin A. Stochastic mechanisms in gene expression. *PNAS*. 1994;94:814–819.
4. Blake WJ, Ern MK, Cantor CR, Collins JJ. Noise in Eukaryotic gene expression. *Nature*. 2003;422:633–637.
5. Elowitz MB, Levine AJ, Siggia ED, Swain PS. Stochastic gene expression in a single cell. *Sci Mag*. 2002;297:1183–1186.
6. Rao NJ, Borwanker JD, Ramkrishna D. Numerical solution of Ito integrations. *SIAM*. 1974;12:393–423.
7. Pardoux E, Talay D. Discretization and simulation of stochastic differential equations. *Acta Appl Math*. 1985;3:23–47.
8. van Kampen NG. *Stochastic Processes in Physics and Chemistry*. North Holland, 1981.
9. Gardiner CW. *Handbook of Stochastic Methods*, 2nd ed. Berlin: Springer, 1985.
10. Gillespie DT. Exact stochastic simulation of couple chemical reactions. *J Chem Phys*. 1977;25:2340–2361.
11. Shah BH, Ramkrishna D, Borwanker JD. Simulation of particulate systems using the concept of the interval of quiescence. *AIChE*. 1977;23:897–904.

12. Cao Y, Gillespie DT, Petzold LR. Efficient step size selection for the tau-leaping simulation method. *J Chem Phys*. 2004.
13. Cao Y, Gillespie DT, Petzold LR. Avoiding negative populations in explicit Poisson tau-leaping. *J Chem Phys*. 2005.
14. Cao Y, Gillespie DT, Petzold LR. Adaptive explitcit-implicit tau-leaping method with automatic tau selection. *J Chem Phys*. 2006; 126:224101.
15. Ramkrishna D, Shu CC, Tran V. New "tau-leap" strategy for accelerated stochastic simulation. *Ind Eng Chem Res*. 2014;53:(49): 18975–18981.
16. Shu CC, Tran V, Ramkrishna D. On speeding up stochastic simulations by parallelization of random number generation. *Chem Eng Sci*. 2015;137:828–836.
17. Peng X, Zhou W, Wang Y. Efficient binomial leap method for simulating chemical kinetics. *J Chem Phys*. 2007;126.
18. Tian T, Burrage K. Binomial leap methods for simulating stochastic chemical kinetics. *J Chem Phys*. 2004;121:10356–10364.
19. Grima R. An effective rate equation approach to reaction kinetics in small volumes: theory and application to biochemical reactions in non-equilibrium steady-state conditions. *J Chem Phys*. 2010;133:(3):35101.
20. Smith S, Cianci C, Grima R. Analytical approximations for spatial stochastic gene expression in single cells and tissues. *Royal Sci*. 2016.
21. Ellis RJ. Macromolecular crowding: an important but neglected aspect of the intracellular environment. *Curr Opin Struct Biol*. 2001; 11(1):114–119.
22. Engblom S, Ferm L, Hellander A, Lotstedt P. Simulation of stochastic reaction-diffusion processes on unstructured meshes. *Tech Rep*. 2008.
23. Erban R, Chapman SJ, Maini P. A practical guide to stochastic simulations of reaction-diffusion processes. arXiv. 2007
24. Isaacson S, Peskin C. Incorporating diffusion in complex geometries into stochastic chemical kinetrics simulations. *SIAM J Sci Comput*. 2006;28:47–74.
25. Ramkrishna D, Amundson NR. *Linear Operator Methods in Chemical Engineering with Applications to Transport and Chemical Reaction System*. Prentice-Hall International, 1985.
26. Amundson NR. *Mathematical Methods in Chemical Engineering: Matrices and Their Application*. New Jersey: Pentice-Hall International, 1966.
27. Kullback S, Leibler RA. On information and sufficiency. Washington DC: *Ann Math Stat*. 1951;22(1):79–86.
28. Kullback S. *Information Theory and Statistics*. Hohn Wiley & Sons, 1959.
29. Kullback S. Letter to the editor: The Kullback-Leibler distance. Washington DC: *Ann Math, Stats*. 1987;41:340–341.
30. Asano T, Wada T, Ohta M, Takigawa. Langevin equation as a stochastic differential equation in nuclear physics. AIP Conf Proc. 2007;891.
31. Kafash B, Lalehzari R, Delavarkhalafi A, Mahmoudi E. Application of stochastic differential system in chemical reactions via simulation. *Math Comput Chem*. 2012;71:265–277.
32. Gillespie DT. The chemical Langevin equation. *J Phys Chem*. 2000; 113:297.
33. Erban R, Chapman SJ. Stochastic modeling of reaction-diffusion processes: algorithms for bimolecular reactions. *Phys Biol*. 2009; 6:4.
34. Isaacson S. The reaction-diffusion master equation as an asymptotic approximation of diffusion to a small target. *SIAM Appl Math*. 2009; 70:77–111.

Manuscript received May 3, 2017, and revision received July 27, 2017.